Neutron Transport Analysis for In-vessel Diagnostics in ITER

Masao Ishikawa, Takashi Kondoh, Takeo Nishitani, Yasunori Kawano, Yoshinori Kusama
Fusion Research and Development Directorate, Japan Atomic Energy Agency, Ibaraki, 311-0193, Japan

(Received: 12 November 2009 / Accepted: 21 January 2010)

Nuclear transport analysis using the MCNP code and heat analysis using a general purpose Finite Element Method code ANSYS 11, respectively, have been carried out for in-vessel components of the microfission chamber (MFC) and the poloidal polarimeter. The nuclear heating rates of the MI cable and the exhaust pipe of the MFC are highest in the gap between two adjacent blanket modules and decrease at greater distances from the gap. Heat analysis using the nuclear heating rate calculation indicates that the maximum temperature of the exhaust pipe can be lowered by changing the distance between two cooling clamps. The nuclear heating rates of the first mirrors of the poloidal polarimeter in the upper port plug are high (> 1 W/cc), and the radiation shield could reduce this rate only by a factor of 2 ~ 4. This heating likely is caused by the effect of streaming neutrons due to an overlap of the beam lines. However, it has been found that the nuclear heating rate can be reduced by reducing the diameter of the beam transmission line.

Keywords: ITER, ITER Diagnostics, MCNP, Neutron Transport Analysis, Nuclear heating, Fusion Power Diagnostics, Neutron Measurement, Microfission Chamber, Polarimeter, Current Profile.

1. Introduction

Neutron transport analysis is very important for the design and optimization of diagnostics in ITER. Especially, in-vessel diagnostics are exposed to strong neutron and gamma radiation that could lead to damage and temperature increases due to the nuclear heating of the components of those diagnostics. A high dose rate due to strong radiation also makes maintenance difficult. Therefore, an evaluation of the neutron/gamma flux, spectrum and nuclear heating at the location of the diagnostics through neutron transport analysis is essential for designing a radiation shield and/or a cooling system.

The microfission chamber (MFC), which is a diagnostic for measuring total neutron source strength in ITER, is one of many in-vessel diagnostics [1]. The MFC for ITER is being developed by the Japanese Domestic Agency (JADA). Heat transport analysis of the MFC based on neutron transport analysis indicates that the detector temperature could be maintained at less than the operational temperature limit without active cooling systems [2]. One of the reasons an active cooling system is unnecessary is that the MFCs are installed behind the blanket module and are not directly exposed to the plasma. However, the double coaxial mineral insulated (MI) cable, which is the signal cable for the MFC, and the exhaust pipe pass through the gap between two blanket modules en route to the upper port [3]. As such, the temperature of the MI cable and the exhaust pipe may increase beyond their operational temperature due to high nuclear heating as a result of the strong radiation of streaming neutrons and gamma rays in the gap. Nuclear heating analysis and heat analysis using MCNP 5 [4] and a general purpose Finite Element Method code ANSYS 11 [5], respectively, have been carried out to design a cooling system consistent with neutron transport calculations.

author's e-mail: ishikawa.masao@jaea.go.jp

Neutron transport analysis for the optical mirrors installed in a port plug is also important to ensure their appropriate operation. The first mirrors have a direct sight-line into the plasma. The poloidal polarimeter, which is also procured by JADA, measures the profile of the toroidal current in the core region using an optical mirror system [6]. The system will be installed in the upper and equatorial ports. It must have a labyrinthine structure to shield the mirrors from neutron/gamma radiation and an active mirror cooling system to offset nuclear heating. In order to design the optimum diagnostics system, a precise estimation of neutron/gamma fluxes, nuclear heating and the dose rate is necessary. In this work, neutron transport analysis also has been carried out on the design of the upper port diagnostics system.

In this paper, results of neutron transport analysis applied to the MFC and the poloidal polarimeter are presented. In section 2, an explanation of the MFC system and results of nuclear heating analysis and heat analysis are presented. Nuclear heating analysis for the optical mirrors of the poloidal polarimeter as well as the explanation of the measurement system is reported in section 3. Finally, a summary is presented in section 4.

2. Neutron transport analysis for the MI cable and the exhaust pipe of the MFC system

2.1 The structure of the MFC system

The MFC is a pencil-sized gas counter containing ^{235}U, which was developed as an in-core monitor for fission reactors. In the MFC, a coating of UO_2 covers the outer cylindrical electrode. The active length is 76 mm, and the MFC contains a total of 10 mg of ^{235}U. The MFC is filled with 95% Ar and 5% N_2 gas at 14.6 atm as an

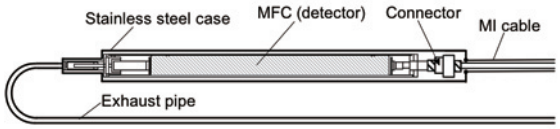

Fig.1 Schematic view of the MFC for preventing Argon gas leakage into the vacuum vessel [3].

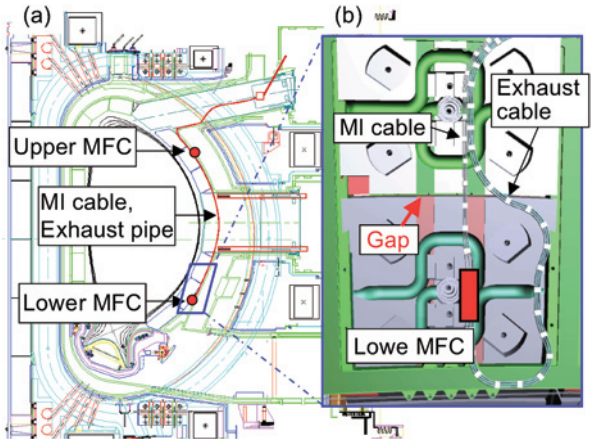

Fig.2 (a) Location of MFCs, MI cable and exhaust pipe on the ITER poloidal cross section and (b) schematic view of those installation positions at the lower outboard location.

ionization gas. In previous design work, an MFC to be applied to the ITER environment was designed as shown in Fig.1. The designed MFC is enclosed in a stainless steel case. The case prevents gas leakage into the vacuum vessel even when Ar gas leaks from the MFC due to any insufficient airtightness of the seal. An exhaust pipe is attached to the stainless steel case in order to exhaust and detect any leaked Ar gas [3]. A tri-axial mineral insulated (MI) cable is used to transfer signals and to supply power to the MFC. The cable uses SiO_2 as an electrical insulator with a packing density of 30%. The central conductor (Cu) is also insulated with a SiO_2 insulator.

MFCs will be installed behind blanket modules at both upper and lower outboard positions in order that the linear combination of output of MFCs at both positions is insensitive to changes in the shape and position of the plasma as shown in Fig.2 [1, 3]. The MI cables and the exhaust cables also will be installed behind blanket modules and travel from each MFC position to the upper port, where the MI cables are connected to a soft cable outside the vacuum vessel via a feed-through in the upper port. The MI cables and the exhaust pipes pass through the gap between blanket modules en route to the upper port as shown in Fig.2 (b).

.

2.2 Nuclear heating analysis for the MI cables and the exhaust pipe

The nuclear heating rates of the MI cables and the exhaust pipe were analyzed through neutron transport calculations using MCNP 5, where FENDL 2.1 [8] was used as the nuclear library for the calculation. A 40° toroidal section which includes the first wall, the blanket

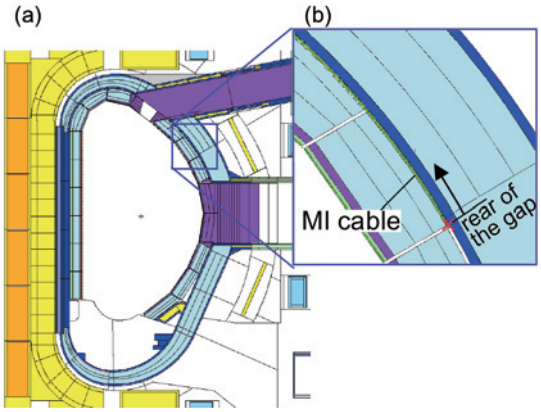

Fig. 3 (a) The poloidal section of MCNP calculation model for nuclear heating calculation of the MI cable and exhaust cable. (B) correspond to those installation locations behind the blanket module.

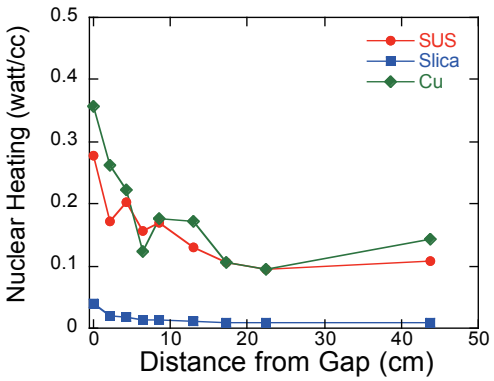

Fig.4 Calculated nuclear heating rate for various distances along the gap from the front reference position (0 cm)

module, the vacuum vessel, poloidal coils and toroidal coils are modeled in this calculation. The poloidal cross-section of this calculation model is shown in Fig.3. The nuclear heating rate of the MI cable and the exhaust pipe behind the blanket modules was modeled as shown in Fig.3 (b). The neutron source is set as a toroidally symmetrical source with 14 MeV, mono-energetic energy, and the neutron profile is set based on the main scenarios of ITER operation (500 MW fusion power). In this calculation, the nuclear heating rate of the MI cable and the exhaust pipe at various distances from the rear of the gap (Fig.3 (b)) in the direction of the arrow has been calculated. Figure 4 shows the calculated nuclear heating rate for each material used for the MI cable (SUS, Silica and CU) and the exhaust pipe (SUS). The horizontal axis in Fig.4 corresponds to the distance from the reference position at the rear of the gap (0 cm) shown in Fig.3 (b). It was found that the nuclear heating rates of SUS and Cu are much higher than that of Silica (the electrical insulator). It was also found that the highest nuclear heating rate is at the rear of the gap, with the nuclear heating rates decreasing as the distance from the gap increases. It is considered that this heating is caused by the ratio of streaming neutrons to the total neutron flux [8].

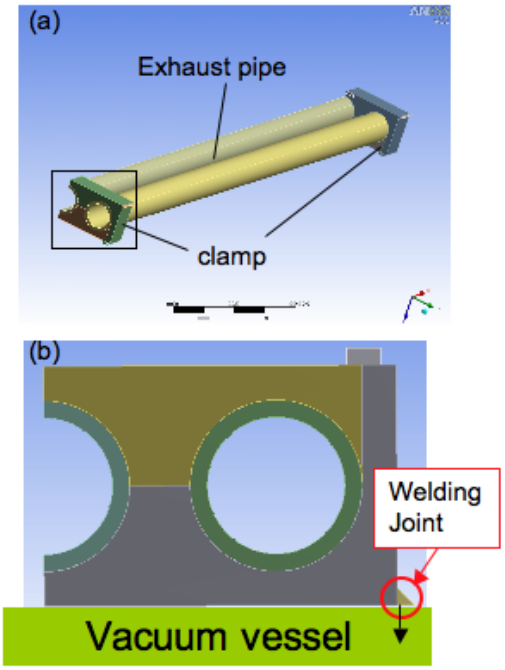

Fig.5 Calculated modes of the heat analysis for the exhaust pipe; (a) whole model, (b) model of the clamp

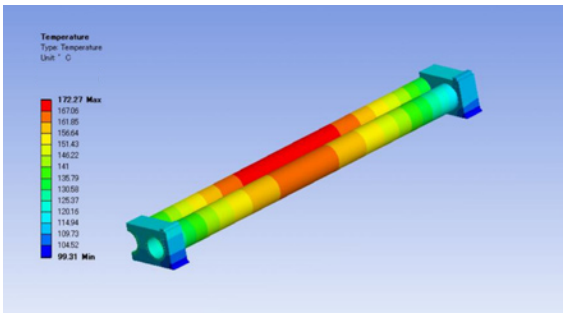

Fig.6 Calculated temperature distribution of the exhaust pipe.

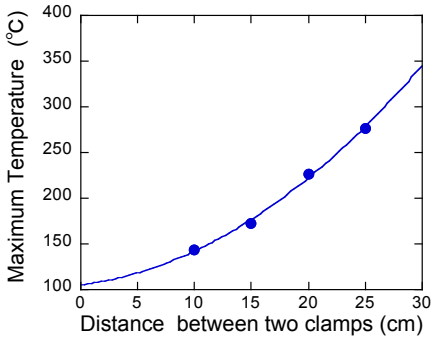

Fig.7 Maximum temperature of the exhaust pipe as a function of the distance between two clamp

2.3 Heat analysis for the exhaust pipe

Heat analysis for the exhaust pipe was carried out using a general purpose Finite Element Method code ANSYS 11, using the calculated nuclear heating rate described in Sec. 2.2. The model for the calculation is shown in Fig.5. In order to offset the nuclear heating of the exhaust pipe, we have designed a clamp as shown in Fig.5 (b). In this calculation, we assumed that the exhaust pipe would be cooled by heat conduction to the vacuum vessel (VV) via only the welding joints on each side of the clamp attached to the VV and that the temperature of the VV would be kept at 100°C.

Figure 6 shows the calculated temperature distribution of the exhaust pipe. The temperature at the center between the two clamps is the highest because that position is farthest from the cooling point of the welding joint of the clamp. Figure 7 shows the maximum temperature as a function of the distance between the two clamps. It was found that the maximum temperature was reduced as the distance between the two clamps shortened. This suggests that the maximum temperature can be controlled by changing the distance between the two clamps. In the future, the distance between the two clamps will be optimized by taking into account thermal expansion, stress and the electromagnetic force of the exhaust pipe.

3. Nuclear heating analysis of the optical mirrors of the poloidal polarimeter

3.1 Measurement system of the poloidal polarimeter

The poloidal polarimeter system consists of two systems of the upper port and the equatorial port diagnostics systems. Each system consists of mirror systems made up of first mirrors, second mirrors and vacuum windows. Far-infrared laser beams (a wavelength of 118 μm) are launched into the plasma through both port plugs using the mirror systems. The laser beams pass through the plasma and are reflected back along the same path by retro-reflectors installed in the first walls. The Faraday rotation angle of a polarization plane of a reflected beam depends on the toroidal current of the plasma. Then, $q(r)$ can be identified using the Faraday rotation angle [6]. In previous design work, view chords of the beam in the upper port system were optimized as listed in table 1. Molybdenum (Mo) was considered one of suitable material of the optical mirror and the diameter of the beam transmission line was optimized 140 mm.

Since the first mirrors are directly exposed to the plasma, strong neutron and gamma radiation could lead to higher nuclear heating and thus, high temperature increases. In order to avoid strong neutron and gamma radiation, a complex optical mirror alignment, which has a labyrinthine structure to shield it from neutrons and a mirror cooling system to offset nuclear heating, is necessary. Therefore, nuclear heating analysis is necessary to design a radiation shield and cooling system for the optical mirror system.

3.2 Nuclear heating analysis of the mirror systems in the Upper port

The nuclear heating rates of the Mo mirrors in the upper port were analyzed using MCNP 5. The basic calculation model is the same as shown in Fig.3. However, the model of the upper port was modified to yield a precise estimation of the nuclear heating rate of the mirrors as shown in Fig.8. In order to estimate how

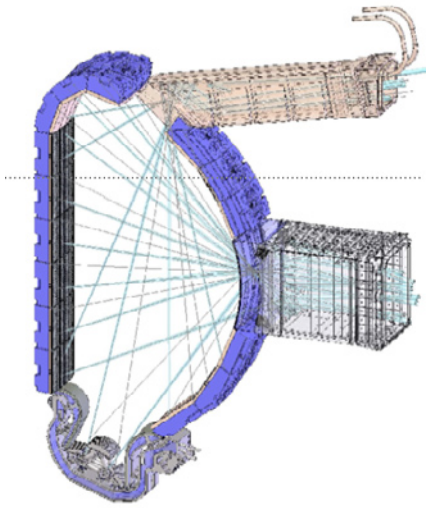

Fig.8 Schmatic view of the Polodal Polarimeter system.

Tab.1 Optimized view chords of the mirrors in the upper port.

	First mirros			Second mirrors		
No.	R (mm)	Z (mm)	Y (mm)	R (mm)	Z (mm)	Y (mm
1	6250	4830	0	7000	4320	80
2	6900	4960	0	7700	4310	−80
3	7180	4980	0	7080	4500	0
4	7950	4915	0	7400	4970	0
5	6450	4870	0	7130	4310	−80
6	6660	4930	0	7520	4290	80

the radiation shield could reduce the nuclear heating rate, the nuclear heating rate of the mirrors was calculated for two cases, one in which the port plug is not filled with any materials, and the other in which the port plug is filled with a neutron shield (70 % stainless steel and 30 % water), absent the mirrors and beam lines (shown in Fig.9 (b)). The calculated nuclear heating rates for both cases are shown in table.2. The nuclear heating rate for the first mirrors is relatively high. Especially affected are those near the plasma (No.1, 2, 3), with rates that exceed 1 w/cc. The radiation shield is estimated to reduce the heating only by a factor of 2 ~ 4 times for the first mirrors (No.1~5). Because these mirrors have direct sight to the plasma center, where is the large neutron and gamma-ray source region, and the radiation shield hardly affect to reduce neutrons and gamma-rays from the plasma center due to streaming neutrons by overlap of the beam transmission lines. On the other hand, even though the mirror No.6 has direct sight to the plasma, the shield can be reduced the nuclear heating rate by more than 1 order. It is considered that the reasons for larger reduction of the nuclear heating than that of No.1 ~3 are that the mirror No.6 doesn't have direct sight to the plasma center and the effect of streaming neutrons much smaller. The nuclear heating rates of the second mirrors are relatively low, and the neutron shield is estimated to reduce the heating rates by more than 1 order (up to more than 2

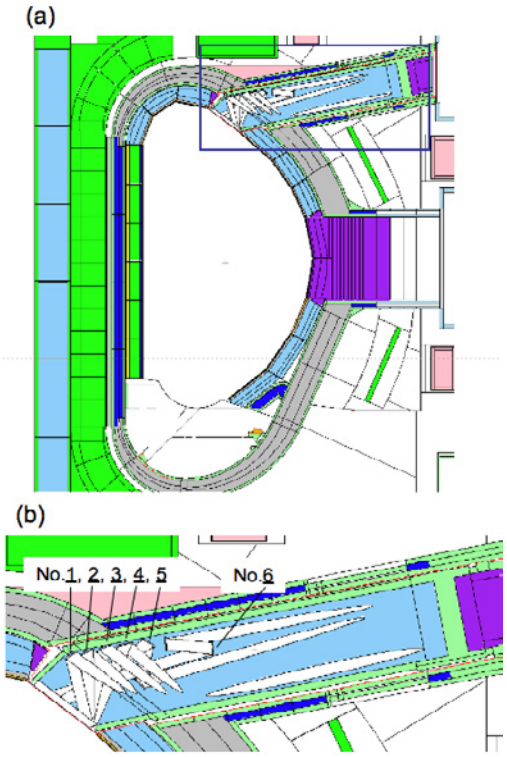

Fig. 9 (a) The poloidal section of MCNP calculation model for nuclear heating calculation of the mirrors of the poloidal polarimenter and (b) correspond to those installation in the upper port. No. 1 ~ 6 corresponds to the first mirror's number, respectively.

orders). In order to investigate any variance in the effect of the streaming neutrons on the nuclear heating of the first mirrors due to an overlap of the beam lines, the role of the diameter of the beam transmission lines on the nuclear heating rate was evaluated by changing the diameter of the beam transmission line in the previous calculation. Figure 10 shows the results of the calculations. It was found that the nuclear heating rate is reduced as the diameter of beam transmission line is reduced. This suggests that one of the ways to suppress nuclear heating is to change the diameter of the beam transmission lines. However, the diameter of the beam transmission line affects measurement accuracy. Optimization of the diameter of the beam transmission lines is therefore necessary.

4. Summary

In this work, neutron transport analysis and heat analysis were performed for MFC and the poloidal polarimeter to assist in the design of a cooling system and radiation shield. The nuclear heating rates of the MI cable and the exhaust pipe of the MFC were calculated using MCNP. The nuclear heating rate of the MI cable and the exhaust pipe of the MFC is highest (0.34, 0.28 w/cc for Cu, SUS) in the gap between blanket modules and decreases as the distance from the gap increases. Heat analysis based on the nuclear heating calculations indicates that temperature increases of the exhaust pipe can be controlled by changing the distance between cooling clamps. The nuclear heating rate of the Mo

Tab.2 Calculated nuclear heating rate of the mirrors of the poloidal polarimeter.

	1st mirror heating (w/cc)		2nd mirror heating (w/cc)	
No.	w/o shiled	with shiled	w/o shiled	with shiled
1	1.97E+00	8.39E-01	9.74E-01	1.50E-01
2	1.59E+00	8.23E-01	7.10E-01	6.63E-02
3	1.18E+00	5.17E-01	2.94E-01	1.41E-02
4	8.66E-01	2.64E-01	2.26E-01	6.48E-03
5	6.46E-01	1.58E-01	9.01E-01	1.06E-01
6	2.25E-01	1.96E-02	4.51E-01	1.37E-02

mirrors of the poloidal polarimeter were also calculated. The nuclear heating rates of the first mirrors are high (> 1 w/cc for mirrors No.1~3), because those are directly exposed to neutron and gamma radiation. The radiation shield (SUS 70% and water 30%) was able to reduce the nuclear heating rate by a factor of only 2 ~ 4 times. It is considered that this rate is caused by the effect of streaming neutrons due to an overlap of the beam lines. Dependence of the diameter of the beam transmission lines on the nuclear heating rate subsequently was evaluated. It was found that the nuclear heating rate could be lowered by reducing the diameter of beam transmission lines. This suggests that one of the ways to suppress nuclear heating is to change the diameter of the beam transmission line.

In this work, heat analysis for the MI cable was not carried out because the thermal conductivity of Silica is unknown. In the future, in order to carry out heat analysis and to design a cooling system for the MI cable, an investigation of the thermal conductivity of the powder and fiber of Silica will be necessary. Detailed estimates of heat transport of the mirrors of the poloidal polarimeter also are necessary to design a radiation shield and cooling system.

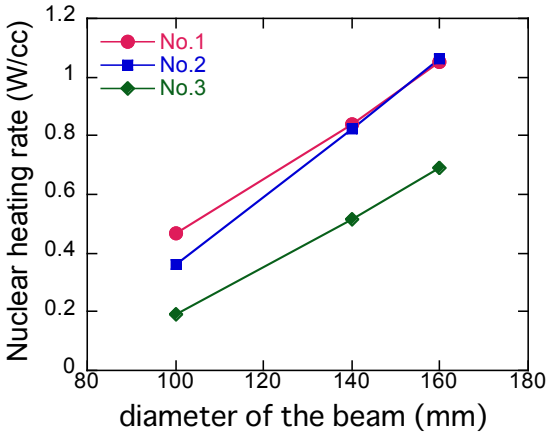

Fig.10 Nuclear heating rate of the first mirrors of the poloidal polarimeter as a function of the diameter of the beam transmission line.

Acknowledgment

The authors would like to acknowledge the ITER JADA team for their help and advice. The authors would like to thank the FNS group in JAEA for their support and advice related to the calculations included in this article.

References

[1] M. Yamauchi et al., Rev. Sci. Instrum., **74** (2003), 1730.
[2] T. Nishitani, et al., Fus. Eng. Des., **82** (2007), 1192.
[3] M. Ishikawa, et al., Plas. Fus. Res. SERIES, **8**(2009), 334
[4] X-5 Monte Carlo Team, "MCNP – A General Monte Carlo N-Particle Transport Code, version 5", LA-UR-03-1987, Los Alamos National Laboratory (2003).
[5] ANSYS Inc., http://www.amsus.com/products/multiphysics.asp
[6] T. Yamaguchi, Plasma Phys. Control. Fusion **50** (2008) 045004.
[7] B. Forrest, A. Trkov, INDC(NDC)-451, IAEA Headquarters, Vienna, Austria (2004).
[8] M. Ishikawa, et al., Rev. Sci. Instrum., **79** (2008), 10E507.